

Control of a Chemical Reactor with Chaotic Dynamics

Rasoulian, Shabnam; Shahrokhi, Mohammad*⁺

*Faculty of Chemical and Petroleum Engineering, Sharif University of Technology,
P.O. Box 11155-9465 Tehran, I.R. IRAN*

Salarieh, Hassan

*Faculty of Mechanical Engineering, Sharif University of Technology,
P.O. Box 11155-9567 Tehran, I.R. IRAN*

ABSTRACT: *In this paper, control of a non-isothermal continuous stirred tank reactor in which two parallel autocatalytic reactions take place has been addressed. The reactor shows chaotic behavior for a certain set of reactor parameters. In order to control the product concentration, an optimal state feedback controller has been designed. Since concentrations of reactor species are not measured, an observer has been designed for implementation of the proposed control scheme. The local asymptotic stability of the closed-loop system including observer dynamics has been shown via the Lyapunov stability theorem. Effectiveness of the proposed controller in load rejection and set point tracking has been illustrated through simulation.*

KEY WORDS: *Chaos, State feedback, Optimal control, Observers, Stability, Chemical reactor.*

INTRODUCTION

A chaotic system is a nonlinear deterministic system that shows a complex behavior. In general, for a certain set of parameter values, a nonlinear system can exhibit oscillations or even chaotic behavior. Chemical systems can have complex dynamics due to their nonlinear nature. There are extensive theoretical and experimental studies indicating presence of complex chaotic behavior in chemical reactions and chemical reactors. *Gray & Scott* have investigated the behavior of an isothermal Continuous Stirred Tank Reactor (CSTR) with autocatalytic reaction [1]. They observed limit cycles and instabilities in such a system [2]. *Lynch et al.* showed that chaotic oscillations are possible in a non-isothermal CSTR

in which two, exothermic, first order, irreversible reactions are taking place in parallel [3]. *Mankin & Hudson* showed that chaos can occur in a forced exothermic chemical reactor [4]. They also showed existence of chaos in two coupled non-isothermal CSTRs [5]. A tutorial review article on the research works regarding this topic up to 1988 is given by *Doherty & Ottino* [6]. An interesting variety of steady state behaviors are also observed in a non-isothermal CSTR [7]. *Pellegrini & Biardi* showed that using a PI controller in a CSTR can lead to chaos [8]. *Perez & Albertos* by changing parameters of the PI controller and cooling water flow rate in a CSTR could generate self oscillation and chaotic

* To whom correspondence should be addressed.

+ E-mail: shahrokhi@sharif.edu

1021-9986/10/4/149

11/\$/3.10

dynamics [9]. Peng *et al.* observed chaotic behavior in a closed three-variable autocatalator [10]. Lynch showed that dynamics of a parallel cubic autocatalator can lead to chaos as the input concentration ratio to the reactor increases [11]. It was also shown that chaos occurs in a mixed cubic and quadratic autocatalytic reaction [12]. Lynch proved that existence of chaotic behavior does not depend on presence of a reaction step involving cubic autocatalysis, and showed that chaotic behavior is preserved when the cubic step is replaced by successive bimolecular steps involving an intermediate [13]. An extended review regarding chaos and its applications in the process system engineering has been made by Lee & Chang [14]. Chaotic behavior is irregular, complex and generally undesirable. Therefore, within the research area of nonlinear dynamics, control of chaos has received increasing attention. Chaos control has been of broad interest since early 1990s. In 1990, Ott *et al.* showed that a chaotic attractor can be converted to one of a large number of possible attracting periodic motions by making only small time dependent perturbations in system parameters [15]. This method is applied to a prototype model for isothermal chemical chaos to stabilize unstable limit cycles out of chaotic behavior [16]. Bandyopadhyay *et al.* have successfully applied this approach to stabilize the dynamics of a chaotic non-isothermal CSTR [17].

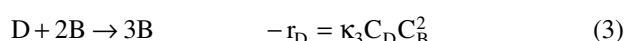
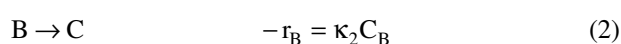
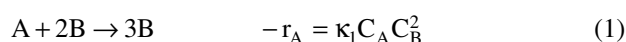
Another method was proposed by Pyragas in which a chaotic system can be stabilized by using proportional delayed feedback [18]. Chaotic dynamics of a set of coupled non-isothermal CSTRs is stabilized using this technique by Chen *et al.* [19]. This method has also been applied to the Belousov-Zhabotinsky (BZ) reaction to stabilize unstable periodic orbits embedded in the chaotic reactors [20]. Another approach for controlling a chaotic process is designing a model based controller. A controller based on internal model control has been designed by Bandyopadhyay *et al.* for a chaotic CSTR [21].

In this paper, it has been shown that a non-isothermal CSTR, in which two parallel autocatalytic reactions take place, may have chaotic behavior. The concentration control has been performed for this reactor through an optimal state feedback with integral action. Since implementation of the proposed controller requires system states, a nonlinear observer has been used for state estimation. The local asymptotic stability of the proposed control scheme including observer dynamics has been

shown and its effectiveness has been demonstrated through simulation.

REACTION KINETICS AND REACTOR MODELING

As described by Lynch an isothermal CSTR composed of two parallel cubic autocatalytic reactions with catalyst decay can produce chaotic dynamics [11-13]. In this work, the non-isothermal version of these reactions has been considered. The reaction kinetics can be written as:



where $\kappa_i = k_i \exp(-E_i/RT)$, $i = 1, 2, 3$.

Reactor mass balances for species A, D and B yield:

$$V \frac{dC_A}{dt} = QC_{A0} - QC_A - \kappa_1 C_A C_B^2 V \quad (4)$$

$$V \frac{dC_D}{dt} = QC_{D0} - QC_D - \kappa_3 C_D C_B^2 V \quad (5)$$

$$V \frac{dC_B}{dt} = QC_{B0} - QC_B + \kappa_1 C_A C_B^2 V - \kappa_2 C_B V + \kappa_3 C_D C_B^2 V \quad (6)$$

Making energy balances for reactor and its jacket gives:

$$\rho V C_p \frac{dT}{dt} = \rho Q C_p (T_0 - T) + R_H (C_A, C_D, C_B, T) + UA(T_j - T) \quad (7)$$

$$\rho_j V_j C_{pj} \frac{dT_j}{dt} = \rho_j Q_j C_{pj} (T_{j0} - T_j) + UA(T - T_j) \quad (8)$$

where:

$$R_H (C_A, C_D, C_B, T) = (-\Delta H_1) \kappa_1 C_A C_B^2 V + (-\Delta H_2) \kappa_2 C_B V + (-\Delta H_3) \kappa_3 C_D C_B^2 V$$

In order to decrease the number of parameters in the above equations and simplify the mathematical model,

Table 1: Dimensionless variables and their definitions.

Dimensionless variable	Definition	Dimensionless variable	Definition	Dimensionless variable	Definition
x_1	C_A/C_{ref}	γ_1	C_{A0}/C_{ref}	Da_1	$Vk_1C_{ref}^2e^{-\varphi}/Q$
x_2	C_D/C_{ref}	γ_2	C_{D0}/C_{ref}	Da_2	$Vk_3C_{ref}^2e^{-\varphi\alpha_2}/Q$
x_3	C_B/C_{ref}	γ_3	C_{B0}/C_{ref}	Da_3	$Vk_2e^{-\varphi\alpha_1}/Q$
x_4	T/T_{ref}	α_1	E_2/E_1	U_1	$UA/\rho QC_p$
x_5	T_j/T_{ref}	α^2	E_3/E_1	U_2	$UA/\rho_j Q_j C_{pj}$
τ	tQ/V	β_1	$(-\Delta H_2)/(-\Delta H_1)$	ζ	T_0/T_{ref}
φ	E_1/RT_{ref}	β_2	$(-\Delta H_3)/(-\Delta H_1)$	u	T_{j0}/T_{ref}
ε	VQ_j/V_jQ	η	$(-\Delta H_1)C_{ref}/\rho C_p T_{ref}$		

the system equations are transformed to a dimensionless form as given below:

$$\frac{dx_1}{d\tau} = \gamma_1 - x_1 - Da_1 x_1 x_3^2 e^{-\varphi\left(\frac{1}{x_4}-1\right)} \quad (9)$$

$$\frac{dx_2}{d\tau} = \gamma_2 - x_2 - Da_2 x_2 x_3^2 e^{-\varphi\alpha_2\left(\frac{1}{x_4}-1\right)} \quad (10)$$

$$\frac{dx_3}{d\tau} = \gamma_3 - x_3 + Da_1 x_1 x_3^2 e^{-\varphi\left(\frac{1}{x_4}-1\right)} - \quad (11)$$

$$Da_3 x_3 e^{-\varphi\alpha_1\left(\frac{1}{x_4}-1\right)} + Da_2 x_2 x_3^2 e^{-\varphi\alpha_2\left(\frac{1}{x_4}-1\right)}$$

$$\frac{dx_4}{d\tau} = \zeta - x_4 + R'_H(x_1, x_2, x_3, x_4) + U_1(x_5 - x_4) \quad (12)$$

$$\frac{dx_5}{d\tau} = \varepsilon(U_2(x_4 - x_5) + u - x_5) \quad (13)$$

where

$$R'_H(x_1, x_2, x_3, x_4) = \eta Da_1 x_1 x_3^2 e^{-\varphi\left(\frac{1}{x_4}-1\right)} + \beta_1 \eta Da_3 x_3^2 e^{-\varphi\alpha_1\left(\frac{1}{x_4}-1\right)} + \beta_2 \eta Da_2 x_2 x_3^2 e^{-\varphi\alpha_2\left(\frac{1}{x_4}-1\right)}$$

The dimensionless variables and model parameters with their definitions are given in Table 1. In this table C_{ref} and T_{ref} are reference values of concentration and temperature respectively.

Through simulation, it has been found that for the following values of system parameters: $\varphi = 8$, $\alpha_1 = 0.8$,

$\alpha_2 = 1.1$, $\eta = 0.375$, $\beta_1 = 0.69$, $\beta_2 = -0.37$, $\gamma_1 = 1.5$, $\gamma_2 = 4.2$, $\gamma_3 = 1$, $Da_1 = 5483.8$, $Da_2 = 108.206$, $Da_3 = 30.913$, $U_1 = 200$, $U_2 = 27$, $\zeta = 1$, $u = 1$, $\varepsilon = 1$, reactor has chaotic dynamics.

The two and three dimensional forms of the attractor are shown in Figs.1 and 2.

Additional details about the structure of the attractor can be provided by examining the Poincare section of the states variables on the transversal surface: $x_1 = 0.025$. The Poincare map of the system shows fractal geometry whose projections on $x_2 - x_3$ and $x_4 - x_5$ surfaces are illustrated in Figs.3 and 4. Lyapunov exponents are the most useful dynamical diagnostic for chaotic systems and usually positive Lyapunov exponents imply chaotic dynamics. As a matter of fact, they quantify the exponential divergence of initially close state space trajectories and estimate the amount of chaos in a system. The method presented by Wolf *et al.* has been used for obtaining the Lyapunov exponents and their variations with respect to time are shown in Fig.5 [22].

As can be seen from Fig.5, system has three negative and one zero Lyapunov exponents and one positive Lyapunov exponent with the value of 1.48.

Chaotic behavior in chemical reactors occurs due to undesirable concentration variations of some components. Control of chaotic reactors is a challenging problem because these variations can lead to thermal runaway.

For the reactor under consideration, the equilibrium point is $x_e = (x_{1e}, x_{2e}, x_{3e}, x_{4e}, x_{5e}) = (0.0222, 1.6892, 0.0595, 1.1819, 1.1754)$. If the dimensionless jacket inlet temperature is chosen as manipulated variable, the model

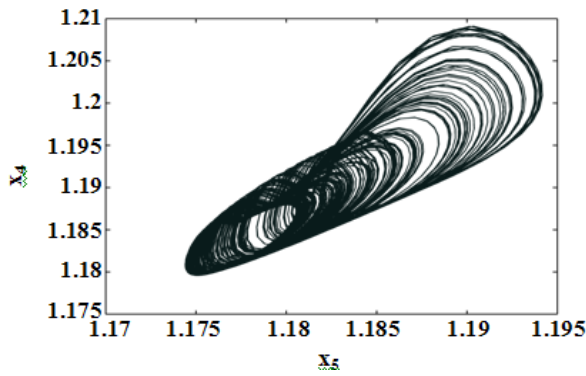


Fig. 1: Two dimensional plot of the attractor, x_4 versus x_5 .

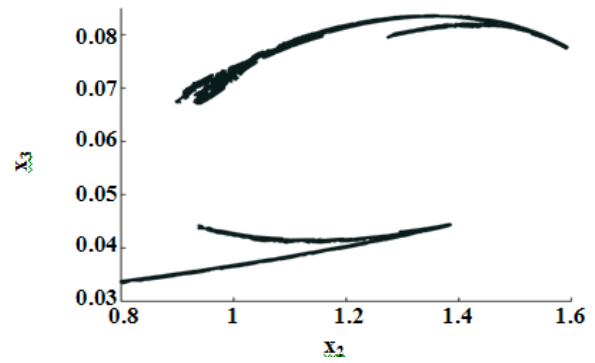


Fig. 3: x_3 versus x_2 on the surface of $x_1 = 0.025$.

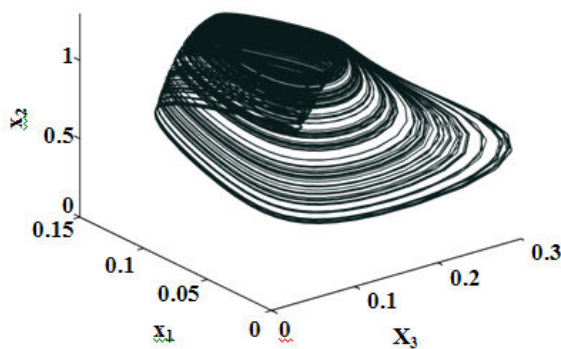


Fig. 2: Three dimensional plot of the attractor.

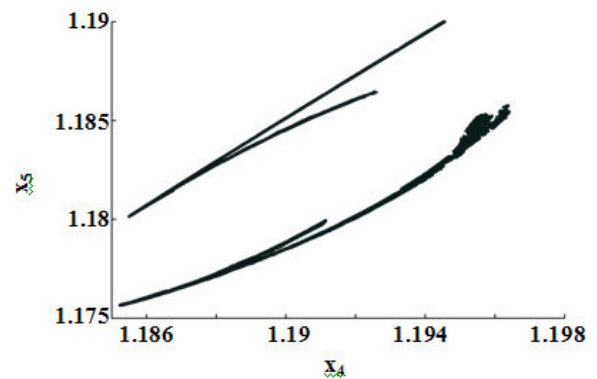


Fig. 4: x_5 versus x_4 on the surface of $x_1 = 0.025$.

can be written in the standard input affine form, as given below:

$$\dot{x} = f(x) + bu \tag{14-a}$$

$$y = cx \tag{14-b}$$

where

$$f(x) = \begin{bmatrix} \gamma_1 - x_1 - Da_1 x_1 x_3^2 e^{-\varphi\left(\frac{1}{x_4}-1\right)} \\ \gamma_2 - x_2 - Da_2 x_2 x_3^2 e^{-\varphi\alpha_2\left(\frac{1}{x_4}-1\right)} \\ \gamma_3 - x_3 - Da_1 x_1 x_3^2 e^{-\varphi\left(\frac{1}{x_4}-1\right)} - \\ Da_3 x_3 e^{-\varphi\alpha_1\left(\frac{1}{x_4}-1\right)} + Da_2 x_2 x_3^2 e^{-\varphi\alpha_2\left(\frac{1}{x_4}-1\right)} \\ \zeta - x_4 + R'_H(x_1, x_2, x_3, x_4) + U_1(x_5 - x_4) \\ \varepsilon(U_2(x_4 - x_5) - x_5) \end{bmatrix} \tag{15}$$

$$b = \begin{bmatrix} 0 \\ 0 \\ 0 \\ 0 \\ 0 \\ \varepsilon \end{bmatrix}, \quad c^T = \begin{bmatrix} 0 \\ 0 \\ 1 \\ 0 \\ 0 \end{bmatrix}$$

The schematic diagram of the process has been shown in Fig.6. Jacket inlet temperature has been used as manipulated variable. In practice by changing hot and cold flow rates, the jacket inlet temperature can be fixed to the desired value. Since control valves have very fast dynamics in comparison to the process, mixing with no dynamics has been assumed.

The main objective of this work is to control the chaotic behavior of the above reactor at its equilibrium point. The unstable limit cycles, due to their cyclic patterns are not desired for a reactor. Therefore it is attempted to stabilize asymptotically the equilibrium point of the system which leads to a steady and uniform concentration of the reactor product. As a first attempt, control of reactor concentration using the traditional PID controller was tested. Since the process has a chaotic behavior, standard tuning techniques like Ziegler-Nicholes method cannot be used. Therefore it was tried to find controller parameters by trial and error. Unfortunately no suitable controller parameters were obtained. As an alternative method, an objective function (integral square of error)

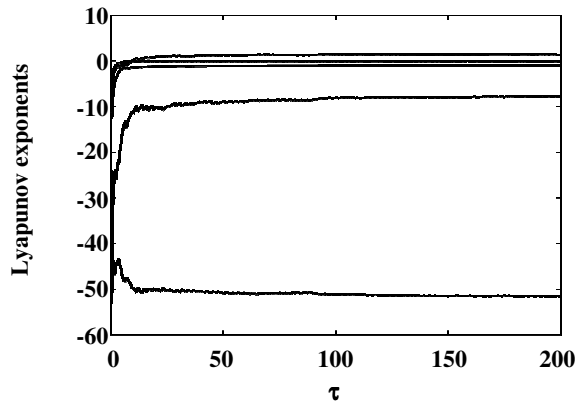


Fig. 5: Convergence of Lyapunov exponents.

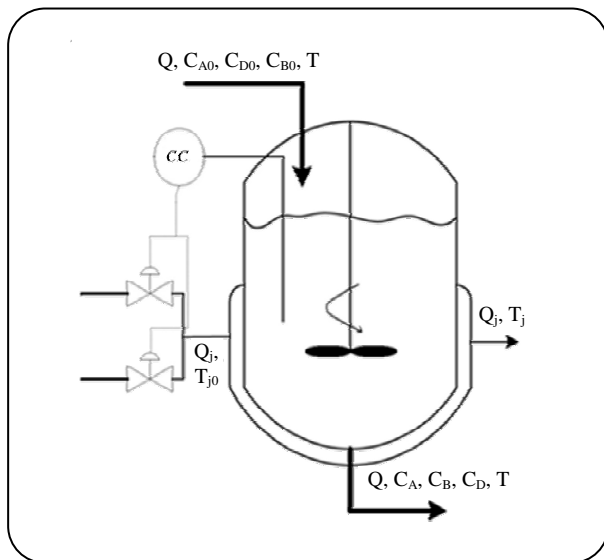


Fig. 6: schematic diagram of the reactor.

was defined and the genetic algorithm was used to minimize this performance index but no feasible set of controller parameters was obtained. Consequently it was tried to apply the feedback linearization method, due to nonlinear nature of the system. Because of some singularities associated with the control action provided with this method, this strategy was not also applicable. Therefore, the linear state feedback control strategy was applied to control the system instead of the Global Linearization Control (GLC) method.

Linearized model

In order to perform stability analysis and controller design, the linearized model around the equilibrium point of Eqs.9-13 is obtained and given below:

$$\dot{x} = Ax + bu \quad (16)$$

where

$$A = \left[\frac{\partial f}{\partial x} \right]_{x=x_e} = \quad (17)$$

$$\begin{pmatrix} -67.5 & 0 & -49.6252 & -8.455 & 0 \\ 0 & -2.484 & -84.2696 & -15.79 & 0 \\ 66.5 & 1.4841 & 50.117 & 1.6829 & 0 \\ 24.9 & -0.206 & 28.3358 & -194.18 & 200 \\ 0 & 0 & 0 & 27 & -28 \end{pmatrix}$$

The eigenvalues of A are $\lambda_1 = -221.4$, $\lambda_2 = -27.6$, $\lambda_{3,4} = 3.98 \pm 17.7i$, $\lambda_5 = -1$. The computed eigenvalues show that, the process is unstable around its equilibrium point.

CONTROLLER DESIGN

In this section, using the linearized model, a controller based on state feedback technique for achieving the desired product composition (x_3) has been proposed. In order to provide feedback controller with integral action on the third state, the time derivative of this state has been set to zero and the resulting equation is augmented into system equations. Controllability matrix of the augmented linearized model, shows that the system is locally controllable. An optimal controller, based on the following objective function, has been designed.

$$J(x(t), u(t)) = \int_0^{\infty} (x^T(t)R_x x(t) + u^T(t)R_u u(t)) dt \quad (18)$$

where R_x and R_u are symmetric, positive semi-definite and positive definite matrices respectively. The optimal input that minimizes the above objective function is given by $u = -kx$, where k is obtained by solving the associated Riccati equation.

OBSERVER DESIGN

Implementation of designed optimal state feedback controller requires system states, while in the most of practical applications only some of the states are available. For the reactor under consideration, it is assumed that only reactor temperature is measured and other states including concentrations of different species and jacket temperature are not available. An observer can be used for estimating the unavailable states. Since f is a locally Lipschitz vector field function, Eq.14 can be written as:

$$\dot{x} = Ax - Ax + f(x) + bu \quad , \quad A = \left. \frac{\partial f}{\partial x} \right|_{x=x_e} \quad (19-a)$$

$$y = cx \quad (19-b)$$

The above equation can be written in the following form:

$$\dot{\hat{x}} = A\hat{x} + \tilde{f}(\hat{x}) + bu + \theta \quad (20-a)$$

$$y = c\hat{x} \quad (20-b)$$

where $\tilde{f}(\hat{x}) = -A\hat{x} + f(\hat{x}) - \theta$ and θ is a constant vector. $\tilde{f}(\hat{x})$ is a locally Lipschitz vector field function such that $\tilde{f}(0) = 0$. If (A, c) is observable, then there exists a vector K such that real parts of all eigenvalues of $A_0 = A - Kc$ are negative. The following observer proposed by Thau has been used [23].

$$\dot{\hat{x}} = A\hat{x} + \tilde{f}(\hat{x}) + bu + K(y - \hat{y}) + \theta \quad (21)$$

Defining the observer error as $\hat{e} = x - \hat{x}$, the observer error dynamics can be described by

$$\dot{\hat{e}} = (A - Kc)\hat{e} + \tilde{f}(x) - \tilde{f}(\hat{x}) = A_0\hat{e} + \tilde{f}(x) - \tilde{f}(x - \hat{e}) \quad (22)$$

Since A_0 is stable, for any symmetric positive definite matrix Q , there is a unique symmetric positive definite matrix P such that

$$A_0^T P + PA_0 = -Q \quad (23)$$

Consider the following Lyapunov function:

$$V = \hat{e}^T P \hat{e} \quad (24)$$

The time derivative of V along the solution of Eq. (22) becomes

$$\dot{V} = -\hat{e}^T Q \hat{e} + 2\hat{e}^T P [\tilde{f}(x) - \tilde{f}(x - \hat{e})] \quad (25)$$

Since \tilde{f} satisfies the Lipschitz condition, the following inequality holds

$$\|\tilde{f}(x_1) - \tilde{f}(x_2)\| \leq L \|x_1 - x_2\| \quad (26)$$

Using inequality (26) in Eq. (25) yields

$$\dot{V} \leq -\hat{e}^T Q \hat{e} + 2L \|\hat{e}\| \|\hat{e}\| \leq (-\lambda_{\min}(Q) + 2L\|P\|) \|\hat{e}\|^2 \quad (27)$$

Hence if

$$L < \frac{\lambda_{\min}(Q)}{2\|P\|} \quad (28)$$

then, the Thau observer is asymptotically stable. In presence of unmeasured disturbance, the observer can be extended to estimate the disturbance along with state estimates. To do this, the observer is augmented to include the observable disturbances.

STABILITY PROOF OF CLOSED LOOP SYSTEM

In this section local stability of the closed loop system including observer dynamics has been shown. If control error is defined as

$$e = x - x_e \quad (29)$$

then, closed loop and observer error dynamics are given by

$$\dot{e} = Ae + o(e^2) + b(u - u_e) \quad (30)$$

$$\dot{\hat{e}} = A_0\hat{e} + \tilde{f}(x) - \tilde{f}(x - \hat{e}) \quad (31)$$

Where $o(e^2)$ indicates the higher order error terms. State feedback control law can be written as $u = -k(e - \hat{e}) + u_e$, where u_e denotes control action at the equilibrium point. Now, consider the following Lyapunov function:

$$V = e^T P_1 e + \hat{e}^T P \hat{e} \quad (32)$$

Where P is obtained from the Lyapunov equation of (23). The time derivative of V becomes

$$\dot{V} = \dot{e}^T P_1 e + e^T P_1 \dot{e} + \dot{\hat{e}}^T P \hat{e} + \hat{e}^T P \dot{\hat{e}} \quad (33)$$

Eq.33 along the solution of Eqs. (30) and (31) is rewritten as:

$$\dot{V} = e^T \left[(A^T - k^T b^T) P_1 + P_1 (A - bk) \right] e + \quad (34)$$

$$\hat{e}^T (A_0^T P + PA_0) \hat{e} + \hat{e}^T k^T b^T P_1 e + e^T P_1 bk \hat{e} + 2\hat{e}^T P (\tilde{f}(x) - \tilde{f}(x - \hat{e})) + O(e^3)$$

Let $A - bk = A_1$, then \dot{V} becomes,

$$\dot{V} = e^T (A_1^T P_1 + P_1 A_1) e + \hat{e}^T (A_0^T P + PA_0) \hat{e} + \quad (35)$$

$$\hat{e}^T k^T b^T P_1 e + e^T P_1 bk \hat{e} + 2\hat{e}^T P (\tilde{f}(x) - \tilde{f}(x - \hat{e})) + O(e^3)$$

Defining $A_1^T P_1 + P_1 A_1 = -Q_1$, $A_0^T P + PA_0 = -Q$, Eq.(35) can be written as

$$\dot{V} = -e^T Q_1 e - \hat{e}^T Q \hat{e} + \hat{e}^T k^T b^T P_1 e + \quad (36)$$

$$e^T P_1 bk \hat{e} + 2\hat{e}^T P (\tilde{f}(x) - \tilde{f}(x - \hat{e})) + O(e^3)$$

According to Rayleigh inequality,

$$\lambda_{\min}(Q) \hat{e}^T \hat{e} \leq \hat{e}^T Q \hat{e} \leq \lambda_{\max}(Q) \hat{e}^T \hat{e} \quad (37)$$

$$\lambda_{\min}(Q_1) e^T e \leq e^T Q_1 e \leq \lambda_{\max}(Q_1) e^T e$$

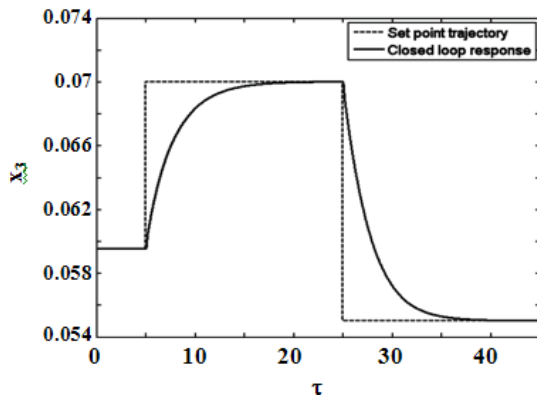


Fig. 7: Set point trajectory and closed loop response of x_3 for set point tracking.

Using inequalities (26) and (37), Eq.(36) can be written as:

$$\dot{V} \leq -\lambda_{\min}(Q_1)\|e\|^2 - \lambda_{\min}(Q_1)\|\hat{e}\|^2 + \quad (38)$$

$$2\|e\|\|P_1\|\|b\|\|k\|\|\hat{e}\| + 2L\|P\|\|e\|^2 + O(e^3)$$

The last term of inequality (38) can be neglected in the vicinity of origin. Defining α, β and γ as $\alpha = -\lambda_{\min}(Q_1)$, $\beta = -\lambda_{\min}(Q) + 2L\|P\|$, $\gamma = 2\|P_1\|\|B\|\|k\|$, inequality (38) can be written as:

$$\dot{V} \leq \begin{pmatrix} \|e\| & \|\hat{e}\| \end{pmatrix} \begin{pmatrix} \alpha & \gamma/2 \\ \gamma/2 & \beta \end{pmatrix} \begin{pmatrix} \|e\| \\ \|\hat{e}\| \end{pmatrix} \quad (39)$$

From the above inequality it is observed that \dot{V} is locally negative definite if:

$$\alpha < 0 \quad \& \quad \gamma^2 < 4\alpha\beta$$

or equivalently,

$$\|P_1\|^2 \|b\|^2 \|k\|^2 < \lambda_{\min}(Q_1)(\lambda_{\min}(Q) - 2L\|P\|) \quad (40)$$

Therefore if Q and Q_1 are chosen such that the above condition is satisfied, the closed loop system including observer dynamics is locally asymptotically stable.

SIMULATION RESULTS

In this section, simulation results are presented to show the effectiveness of the proposed controller. To make the simulations more realistic, actuator constraint has been taken into account and it is assumed that the jacket inlet temperature can be changed between 93% and 122%

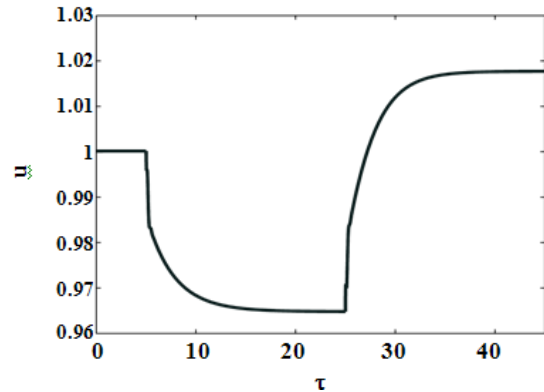


Fig. 8: Control action for x_3 set point tracking.

of reference temperature. For controller design, the weight matrices were chosen as given below:

$$R_x = \begin{pmatrix} 10 & 0 & 0 & 0 & 0 & 0 \\ 0 & 10 & 0 & 0 & 0 & 0 \\ 0 & 0 & 300 & 0 & 0 & 0 \\ 0 & 0 & 0 & 10 & 0 & 0 \\ 0 & 0 & 0 & 0 & 10 & 0 \\ 0 & 0 & 0 & 0 & 0 & 400 \end{pmatrix}, \quad R_u = 1$$

For these weight matrices the controller gain is $k = [-65.9105, -7.5989, -58.6105, 7.2008, 32.6163, -20]$.

To check the performance of the control scheme in the absence of observer dynamics, first it is assumed that all states are available. First the proposed controller is tested for set point tracking. As shown in Fig. 7, the desired trajectory has been well tracked. The corresponding control action is shown in Fig. 8.

In what follows, effect of disturbance on the closed loop response has been studied. One of the common loads is variation of feed concentration. Therefore γ_1 has been considered as the main disturbance for this process. Simulation result when γ_1 changes from 1.5 to 1.45 at $\tau=5$ and next to 1.4 at $\tau=25$ is shown in Fig. 9. As can be seen, loads are rejected satisfactorily. The corresponding control action has been depicted in Fig. 10.

So far, it has been assumed that all states are available, but this is not the case in practice. Concentration measurement is difficult and usually has time lag. It can be shown that the system is observable through reactor temperature measurements. Based on availability of reactor temperature measurements,

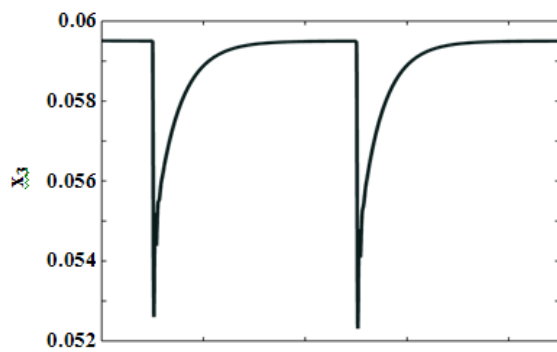


Fig. 9: Closed loop response of x_3 for disturbance in γ .

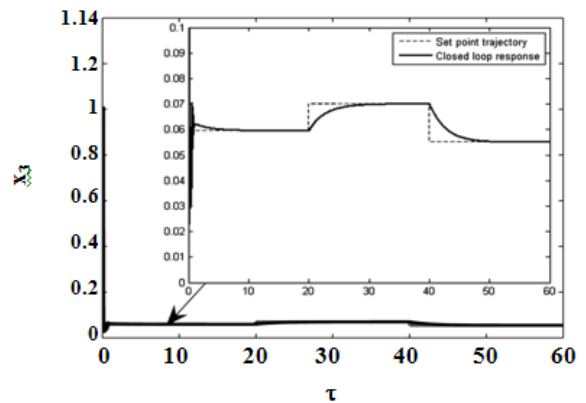


Fig. 11: Set point trajectory and closed loop response of x_3 for set point tracking using observer.

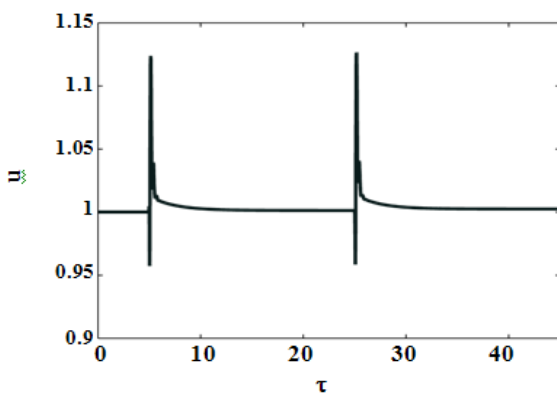


Fig. 10: Control action for x_3 for disturbance rejection.

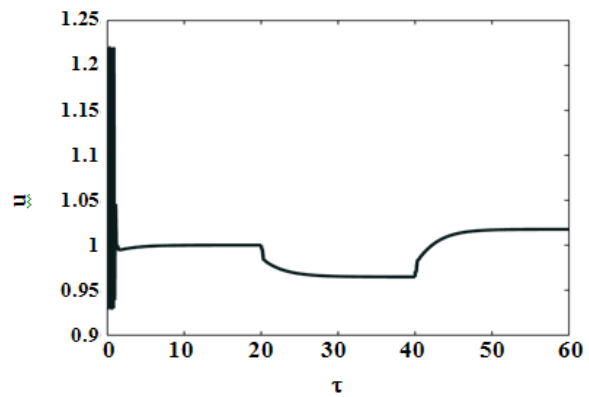


Fig. 12: Control action for x_3 set point tracking using observer.

an observer has been designed. Besides system states, the feed concentration, is also estimated using an augmented observer. In all simulations, the initial values of state estimates and feed composition estimate are set to $[\hat{x}_{10}, \hat{x}_{20}, \hat{x}_{30}, \hat{x}_{40}, \hat{x}_{50}, \hat{\gamma}_{10}]^T = [0.05, 1.9, 0.03, 1, 1, 1.5]^T$. The observer gain, K , has been determined such that poles of observer are placed to $\{-19, -19.5, -20, -20.5, -21, -21.5\}$ and correspondingly the observer gain is $K = [-83.0687, -218.8907, 135.3364, -120.5511, 27.0704, 418.7773]^T$.

First, set point tracking performance of the proposed controller using the designed observer is investigated. As shown in Fig.11 the desired trajectory has been well tracked. The corresponding control action is shown in Fig. 12.

The estimation errors of desired product composition and feed concentration are shown in Figs. 13 and 14. As can be seen, both errors have converged to zero.

Finally, the load rejection performance of the proposed controller in presence of observer is investigated. In order to test the load rejection performance, γ_1 is changed from 1.5 to 1.45 at $\tau=20$ and next to 1.4 at $\tau=40$. The closed loop response of x_3 is shown in Fig.15. As can be seen loads are rejected fairly well. The corresponding control action is shown in Fig.16. The estimation errors of desired product composition and feed concentration are shown in Figs.17 and 18 respectively. As can be seen both errors have converged to zero.

The simulation results indicate that the optimal state feedback controller has a good performance in load rejection and set point tracking when the system state variables are available. When the system states are not measured, they can be estimated by designing an observer. Simulation results indicate that the designed observer has a good performance and the system states are estimated pretty fast. Besides the system states, the feed concentration, is also estimated using an augmented observer.

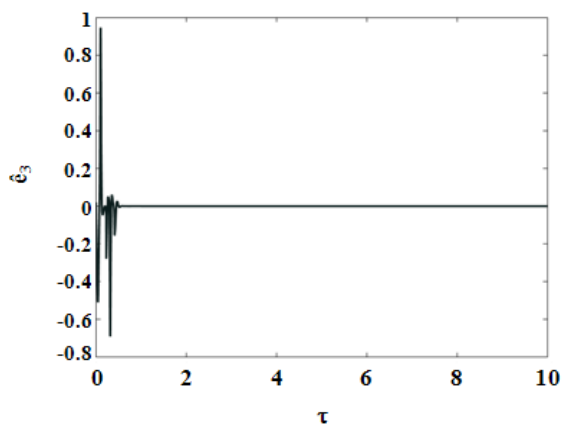


Fig. 13: Estimation error of x_3 in set point tracking.

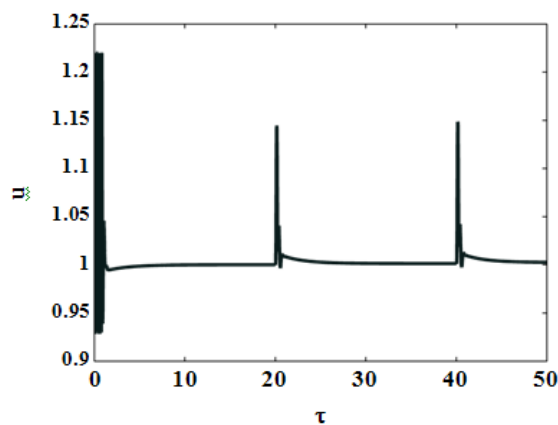


Fig. 16: Control action for x_3 for load rejection using observer.

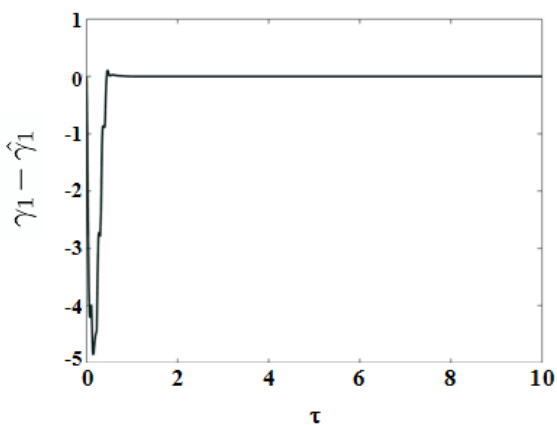


Fig. 14: Estimation error of feed composition in set point tracking.

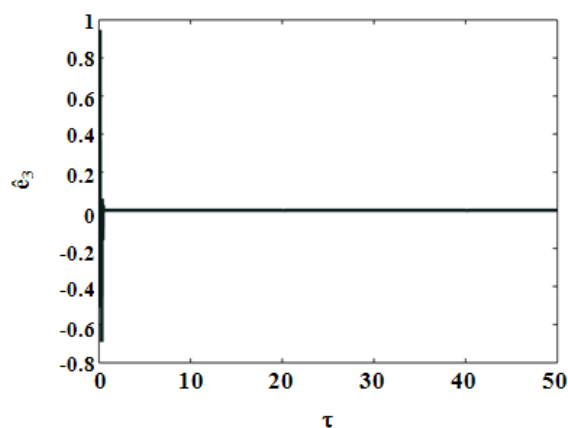


Fig. 17: Estimation error of x_3 in load rejection.

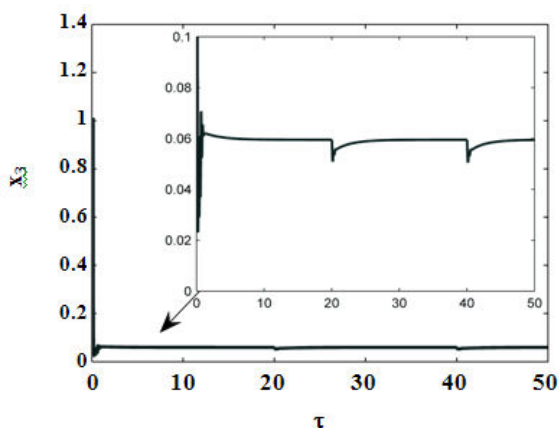


Fig. 15: Closed loop response of x_3 for load rejection using observer.

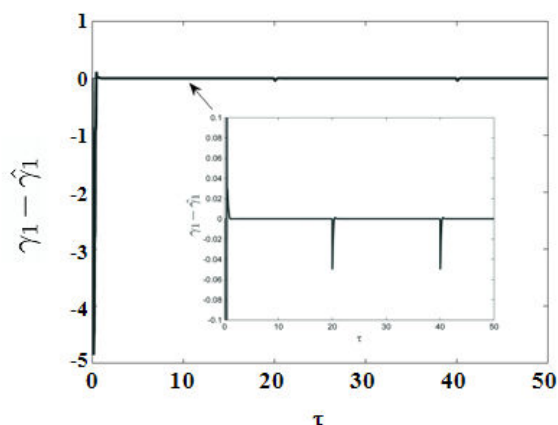


Fig. 18: Error of feed composition estimate in load rejection.

The controller performance is also satisfactory when it is coupled with the state estimator.

CONCLUSIONS

In this paper, a non-isothermal version of Lynch's autocatalytic reactions has been modeled using mass and energy balances. Simulation results indicate that, the reactor has a chaotic behavior for a certain set of parameter values. An observer based controller possessing integral action has been designed to provide off-set free control of desired product concentration. The Lyapunov stability theorem is used to establish local asymptotic stability of closed loop system including observer dynamics. It has been shown that the proposed controller has good set point tracking and load rejection performances.

NOMENCLATURE

A	Heat transfer area
C_A, C_D, C_B	Concentrations of A, D and B in the reactor
C_{A0}, C_{D0}, C_{B0}	Concentrations of A, D and B in the reactor feed
C_p	Solution heat capacity
C_{pj}	Jacket fluid heat capacity
E_1, E_2, E_3	Activation energies
k_1, k_2, k_3	Reaction constants
Q	Flow rate through reactor
Q_j	Jacket flow rate
R	Ideal gas constant
t	Time
T	Reactor temperature
T_j	Jacket temperature
T_0	Feed temperature
T_{j0}	Jacket inlet temperature
U	Heat transfer coefficient
V	Reactor volume
V_j	Jacket volume

Greek letters

$\Delta H_1, \Delta H_2, \Delta H_3$	Heat of reactions
ρ	Solution density
ρ_j	Jacket fluid density

REFERENCES

- [1] Gray P., Scott S.K., Autocatalytic Reactions in the Isothermal, Continuous Stirred Tank Reactor, Isolates and other forms of Multistability, *Chemical Engineering Science.*, **38**, p. 29 (1983).
- [2] Gray P., Scott S.K., Autocatalytic Reactions in the Isothermal Continuous Stirred Tank Reactor, Oscillations and Instabilities in the System $A+2B \rightarrow 3B$; $B \rightarrow C$, *Chemical Engineering Science.*, **39**, p. 1087 (1984).
- [3] Lynch D.T., Rogers T.D., Wanke S.E., Chaos in a Continuous Stirred Tank Reactor, *Mathematical Modelling.*, **3**, p. 103 (1982).
- [4] Mankin J.C., Hudson J.L., Oscillatory and Chaotic Behavior of a Forced Exothermic Chemical Reaction., *Chemical Engineering Science.*, **39**, p. 1807 (1984).
- [5] Mankin J.C., Hudson J.L., The Dynamics of Coupled Nonisothermal Continuous Stirred Tank Reactors, *Chemical Engineering Science.*, **41**, p. 2651 (1986).
- [6] Doherty M.F., Ottino J.M., Chaos in Deterministic Systems: Strange Attractors, Turbulence, and Applications in Chemical Engineering, *Chemical Engineering Science.*, **43**, p. 139 (1988).
- [7] Kay S.R., Scott S.K., Tomlin A.S., Quadratic Autocatalysis in a Non-Isothermal CSTR, *Chemical Engineering Science.*, **44**, p. 1129 (1989).
- [8] Pellegrini L., Biardi G., Chaotic Behavior of a Controlled CSTR, *Computers & Chemical Engineering.*, **14**, p. 1237 (1990).
- [9] Perez M., Albertos P., Self Oscillating and Chaotic Behavior of a PI Controlled CSTR with Control Valve Saturation, *Journal of Process Control.*, **14**, p. 51 (2004).
- [10] Peng B., Scott S.K., Showalter K., Period Doubling and Chaos in a Three Variable Autocatalator, *The Journal of Physical Chemistry.*, **94**, p. 5243 (1990).
- [11] Lynch D.T., Chaotic Behavior of Reaction Systems: Parallel Cubic Autocatalators, *Chemical Engineering Science.*, **47**, p. 347 (1992).
- [12] Lynch D.T., Chaotic Behavior of Reaction Systems: Mixed Cubic and Quadratic Autocatalysis, *Chemical Engineering Science.*, **47**, p. 4435 (1992).
- [13] Lynch D.T., Chaotic Behavior of Reaction Systems: Consecutive Quadratic/Cubic Autocatalysis via Intermediates, *Chemical Engineering Science.*, **48**, p. 2103 (1993).

Received : Dec. 20, 2009 ; Accepted : July 14, 2010

- [14] Lee J.S., Chang K.S., Applications of Chaos and Fractals in Process Systems Engineering, *Journal of Process Control.*, **6**, p. 71 (1996).
- [15] Ott E., Grebogi C., Yorke J.A., Controlling Chaos, *Physical Review Letters.*, **64**, p. 1196 (1990).
- [16] Peng B., Petrov V., Showalter K., Controlling Chemical Chaos, *The Journal of Physical Chemistry.*, **95**, p. 4957 (1991).
- [17] Bandyopadhyay J.K., Ravi Kumar V., Kulkarni B.D., Regulatory Control of a Chaotic Nonisothermal CSTR, *A.I.Ch.E. Journal.*, **39**, p.908 (1993).
- [18] Pyragas K., Continuous Control of Chaos by Self Controlling Feedback, *Physical Letters A.*, **170**, p. 421 (1992).
- [19] Chen C.C., Fu C.C., Tsai C.H., Stabilized Chaotic Dynamics of Coupled Nonisothermal CSTRs, *Chemical Engineering Science.*, **51**, p. 5159 (1996).
- [20] Schneider F.W., Blittersdorf R., Foerster A., Hauck T., Lebender D., Muller J., Continuous Control of Chemical Chaos by Time Delayed Feedback, *The Journal of Physical Chemistry.*, **97**, p. 12244 (1993).
- [21] Bandyopadhyay J.K., Ravi Kumar V., Kulkarni B.D., Deshpande P.B., On Dynamic Control of Chaos: a Study with Reference to a Reacting System, *Physics Letters A.*, **166**, p. 197 (1992).
- [22] Wolf A., Swift J.B., Swinney H.L., Vastano J.A., Determining Lyapunov Exponents from a Time Series, *Physica D.*, **16**, p. 285 (1985).
- [23] Thau F.E., Observing the States of Nonlinear Dynamic Systems, *International Journal of Control.*, **17**, p. 471 (1973).